Research Paper

Increased Transport of Resveratrol Across Monolayers of the Human Intestinal Caco-2 Cells is Mediated by Inhibition and Saturation of Metabolites

Alexandra Maier-Salamon,[1] Birgit Hagenauer,[1] Michael Wirth,[2] Franz Gabor,[2] Thomas Szekeres,[3] and Walter Jäger[1,4]

Purpose. The study's aim was to investigate the dose-dependent effect of sulfation and glucuronidation on intestinal absorption of resveratrol, a dietary constituent found in grapes and various medical plants.

Materials and Methods. The intestinal epithelial membrane transport kinetics and metabolism of resveratrol (10–200 μM) was studied using Caco-2 monolayers cultured in Transwells.

Results. Along with resveratrol it was possible to identify three metabolites, namely, resveratrol-4′-O-glucuronide (M1), resveratrol 3-O-gucuronide (M2), and resveratrol-3-O-sulfate (M3) by LC/MS and NMR. Efflux of the glucuronides M1 and M2 followed Michaelis–Menten kinetics significantly favouring basolateral efflux. The predominant metabolite was the monosulfate M3, however, its formation was strongly inhibited at higher resveratrol concentrations. As biotransformation was either inhibited or saturated, total amount of resveratrol transported across the Caco-2 monolayers increased as much as 3.5-fold at 200 μM resveratrol. This value might be even higher when taking into account the high intracellular concentration of resveratrol, which accounted for up to 61% of the applied dose.

Conclusions. Our data demonstrate a concentration-dependent biotransformation of resveratrol in Caco-2 cells, which may also apply to human enterocytes affecting oral bioavailability.

KEY WORDS: Caco-2 cells; glucuronidation; resveratrol; sulfation; transport.

INTRODUCTION

Resveratrol (resveratrol), *trans*-3,5,4′-trihydroxystilbene, is a dietary constituent found in grapes, peanuts, and a variety of medical plants, which exerts a variety of biological and pharmacological activities including antibacterial, anti-fungal, and cancer protective activities (1,2). It has also been shown to be a non-selective inhibitor of COX-1 and COX-2 and exhibits pronounced antioxidant properties with its ability to inhibit hydrogen peroxide- or lipid hydroperoxide-dependent lipid peroxidation of cellular membrane lipids (3–5). Moreover, resveratrol reduces metal ion-dependent and -independent oxidation of low-density lipoproteins (6,7), a process that is responsible for promoting atherogenesis. It also effectively protects isolated rat hearts from ischemia reperfusion injuries (8,9) reducing myocardial infarct size in comparison with control rat hearts (10). Due to these experimental findings, resveratrol in red wine was deemed responsible for the French paradox, the fact that the incidence of heart infarction in Southern France is 40% lower than in the rest of Europe despite the population's high-fat diet (11).

Studies conducted in rodent models showed a very low oral bioavailability based on extensive metabolism to *trans*-resveratrol-3-O-glucuronide and *trans*-resveratrol-3-O-sulfate (12,13). Following oral administration of resveratrol to mice, the concentration of resveratrol-3-O-sulfate in the serum was approximately threefold higher than the concentration of resveratrol-3-O-glucuronide (12). Only traces of unconjugated resveratrol were observed. The observation that the oral bioavailability of resveratrol is negligible in animals matches the findings in a previous preliminary study in four human subjects receiving an oral dose of 25 mg (14). In a very recent study, Walle *et al.* were also able to observe only trace amounts (<5 ng/ml) of unconjugated resveratrol in plasma samples after administration of 25 mg ^{14}C-resveratrol to six healthy human subjects, although based on urinary excretion data, absorption of total resveratrol (resveratrol plus metabolites) appears to be at least 70%. As observed in the animal studies, this study also revealed the existence of resveratrol monosulfate, presumably resveratrol-3-O-sulfate, as the main metabolite in the plasma and the existence of resveratrol monosulfate and two unidentified monoglucuronides

[1] Department of Clinical Pharmacy and Diagnostics, University of Vienna, A-1090, Vienna, Austria.

[2] Department of Pharmaceutical Technology and Biopharmaceutics, University of Vienna, A-1090, Vienna, Austria.

[3] Clinical Institute for Medical and Chemical Laboratory Diagnostics, Medical University of Vienna, A-1090, Vienna, Austria.

[4] To whom correspondence should be addressed. (e-mail: walter. jaeger@univie.ac.at)

ABBREVIATIONS: AP, apical; BL, basolateral; Cl_i, intrinsic clearance; HPLC, high pressure liquid chromatography; K_i, inhibition constant; K_m, Michaelis constant; MRP, multidrug resistance protein; P_{app}, permeability coefficient; P-gp, P-glycoprotein; TEER, transepithelial electrical resistance; V_{max}, maximal secretion rate.

in the urine. No evidence of enzymatic oxidation of resveratrol could be found in plasma samples (15). The extremely rapid formation of resveratrol monosulfate either after i.v. or oral doses indicates that sulfation might be the main rate-limiting step in resveratrol bioavailability. The pattern of metabolite formation in humans, however, is influenced by the oral dose as in a very recent study only 3-O- and 4′-O-glucuronide but not resveratrol-3-O-sulfate could be identified in the plasma of volunteers after a single oral dose of 1 g (16).

Both liver and gut seem to be involved in resveratrol conjugation as De Santi *et al.* found similar sulfation rates in human liver and duodenum (17). Glucuronidation of resveratrol was also observed in transport studies using human Caco-2 colonic adenocarcinoma cells showing higher concentrations of resveratrol-3-O-sulfate than resveratrol-3-O-glucuronide (18,19)—at least when resveratrol concentrations did not exceed 40 µM. Interestingly, the apical to basolateral transport rate more than doubled when resveratrol concentrations increased from 5 to 40 µM. Whether this increased transport of resveratrol is due to inhibition of metabolite formation or due to decreased intracellular accumulation was not shown. In the present work we therefore investigated the concentration-dependent formation of resveratrol conjugates in Caco-2 cells. Furthermore, the influence of biotransformation, and more importantly, the inhibition of glucuronide and sulfate formation on transepithelial transport of unconjugated resveratrol should be elucidated in order to gain a better understanding of its oral absorption.

MATERIALS AND METHODS

Materials

Resveratrol (3,4′,5-trihydroxy-*trans*-stilbene), sulfatase type V from Limpets (Patella vulgata), Dulbecco's modified Eagle's medium (DMEM), Hank's balanced salt solution (HBSS), and other cell culture components were purchased from Sigma-Aldrich (St. Louis, MO). Methanol and water were of HPLC grade (Merck, Darmstadt, Germany). Fetal bovine serum was obtained from PAA-Biologics, Linz, Austria. All other chemicals and solvents were commercially available, of analytical grade, and used without further purification.

Cell Culture

The human colon adenocarcinoma cell line Caco-2 (American Type Culture Collection, Rockville, MD) was maintained in DMEM supplemented with 10% FBS, 4 mM glutamine and gentamicine (150 µg/ml) in an atmosphere of 5% CO_2 and 95% relative humidity. For transport studies, cells were seeded on 12 mm i.d. polycarbonate filter (0.4 µM pore size) culture inserts (Transwell® Costar, High Wycombe, U.K.) at a density of 6 × 10^4 cells/cm and cultured for 21 days. The integrity of the cell monolayers was determined by measuring the transepithelial electrical resistance (TEER) with a Milicell ERS volt/ohmmeter (Millipore, USA). The cell layers were used for experiments when the TEER exceeded 300 Ω/cm.

Transport and Metabolism Studies

The cell layers were washed twice with HBBS buffer, placed into 12 well plates and equilibrated for 30 min. Resveratrol was dissolved in DMSO and diluted with HBSS buffer (final DMSO concentration <0.5%) to 5–200 µM. Blank experiments contained DMSO in HBSS buffer in place of resveratrol. The loading solutions were applied to either the apical or the basolateral chamber (0.5 and 1.5 ml, respectively) and HBBS served as acceptor medium. Samples (50 µl) from both chambers were taken at the start of the experiment as well as after 1, 3, and 5 hours without replacement of buffer and subsequently analyzed by HPLC. Experiments were carried out in triplicate.

After finishing the transport study, cells were scraped off and washed three times with HBSS buffer. After addition of 0.45 ml HBSS buffer, cells were lysed by repeated (three times) shock freezing in liquid nitrogen and thawing. After centrifugation at 10,000 ×g for 5 min, 100 µl of the supernatant (cytoplasm) was analyzed by HPLC. During the transport experiments the integrity of the monolayers was tested by measuring the TEER. In separate experiments the efflux inhibitors verapamil (40 µM) and cyclosporine (5 µM) were added to the loading solution and applied simultaneously with resveratrol under identical conditions as described above.

Biochemical Synthesis of Resveratrol Metabolites

Livers of male Wistar rats (223–261 g), raised at the Institut für Versuchstierzucht und -haltung (University of Vienna, Himberg, Austria), were perfused with 20 µM of *trans*-resveratrol in a recirculating system as described previously. (19) Bile samples were collected over a time period of 60 min. Bile samples (360–600 µl) were diluted with distilled water (1:2; v/v) and aliquots (200 µl) were injected onto a Hypersil C18 column (10 µm, 250 × 10 mm I.D., Astmoor, England) preceded by a Hypersil -C18 guard column (10 µm, 10 × 3 mm I.D.) at a low-rate of 5 ml/min. Mobile phase and gradient were identical to those used in the analytical HPLC assay (see below). The peaks corresponding to *trans*-resveratrol-3-O-glucuronide and *trans*-resveratrol-3-sulfate from each chromatographic run were collected, pooled, and lyophilized. Structures were confirmed by nuclear magnetic resonance (NMR) measurements. Spectra were recorded on a Varian UnityInova (Varian, Palo Alto, CA) 600 MHz instrument obtaining the following data. The proton shifts of the two metabolites were almost identical with values reported in the literature (12).

Trans-Resveratrol-3-O-Glucuronide

1H NMR (CD_3OD) δ 6.77 (d, *J* 8.6 Hz, H-3′,5′), 7.36 (d, *J* 8.6 Hz, H-2′,6′), 6.98 (d, *J* 6.5 Hz, *trans*-vinyl), 6.85 (d, *J* 16.5 Hz, *trans*-vinyl), 6.77 (tr, *J* 1.9 Hz, H-6), 6.52 (tr, *J* 1.9 Hz, H-4), 6.62 (tr, *J* 1.9 Hz, H-2).

Trans-Resveratrol-3-Sulfate

1H NMR (CD3OD) δ 6.80 (d, *J* 8.5 Hz, H-3′,5′), 7.38 (d, *J* 8.5 Hz, H-2′,6′), 7.06 (d, *J* 16.3 Hz, *trans*-vinyl), 6.90 (d, *J*

16.3 Hz, *trans*-vinyl), 6.77 (tr, *J* 1.7 Hz, H-6), 6.69 (tr, *J* 1.7 Hz, H-4), 7.01 (tr, *J* 1.7 Hz, H-2).

HPLC Analysis

The determination of resveratrol and its metabolites was performed using a Merck "La Chrom" System (Merck, Darmstadt, Germany) equipped with an L-7250 injector, an L-7100 pump, an L-7300 column oven (set at 15°C), a D-7000 interface, and an L-7400 UV-detector (set at a wavelength at 307 nm). Chromatographic separation of resveratrol and its metabolites was performed on a Hypersil BDS-C_{18} column (5 μm, 250 × 4.6 mm I.D. Astmoor, England), preceded by a Hypersil BDS-C_{18} precolumn (5 μm, 10 × 4.6 mm I.D.), at a flow rate of 1 ml/min. The mobile phase consisted of a continuous gradient, mixed from 5 mM ammonium acetate/acetic acid buffer, pH 7.4 (mobile phase A), and methanol (mobile phase B), to elute resveratrol and its metabolites according to their lipophilicity. The mobile phase was filtered through a 0.45 μM filter (HVLP04700, Milipore, Vienna, Austria). The gradient ranged from 10% methanol (0 min) to 20% B at 10 min and linearly increased to 35% B at 22 min, followed by another increase to 60% B at 25 min, where it remained constant until 30 min. Subsequently, the percentage of methanol was decreased within 2 min to 10% in order to equilibrate the column for 8 min before application of the next sample. Calibration of the chromatogram was accomplished using the external standard method. Linear calibration curves were performed from the peak area of resveratrol, resveratrol-3-O-glucuronide, and resveratrol-3-O-sulfate to the external standards resveratrol, resveratrol-3-O-glucuronide, and resveratrol-3-O-sulfate using standard solutions of these compounds to give a concentration range of 0.05 to 10 μg/ml. As a standard for resveratrol-4′-O-glucuronide was not available, quantification of this conjugate was based on the assumption that the molar extinction coefficient of resveratrol-4′-O-glucuronide is similar to resveratrol-3-O-glucuronide.

Structural Identification of Resveratrol Metabolites in Caco-2 Cells

Samples taken from the basolateral compartment (100 μl), 5 h after apical loading were incubated with either 200 units β-glucuronidase or 20 units sulfatase for 24 h at 37°C and subjected to HPLC analysis. Control samples were incubated in the absence of enzymes. To discriminate between mono- and disulfation of resveratrol, liquid chromatography–mass spectrometry (LC/MS) measurements were performed using an HPLC system fitted with an LC200 pump, a 235C DAD detector, and a 200 autosampler (PerkinElmer Sciex Instruments, Wellesley, MA). The system was coupled in line to an API 150Ex mass selective detector (PerkinElmer Sciex) fitted with an atmospheric pressure ionization source for electrospray ionization in the negative mode. The operating conditions were as follows: capillary voltage, −4.00 kV; orifice voltage, −40 V; and gas temperature 400°C. Column, mobile phase, gradient, flow rate, and injection volume were identical to those used in the analytical HPLC assay (see above). The confirmation of resveratrol metabolites in Caco-2 samples was based on their

retention times and ion fragmentation in the MS mode, as compared with those standards available isolated from rat bile.

Data Analyses

For characterization of the transport of resveratrol across Caco-2 monolayers, resveratrol concentrations were varied up to 200 μM. Transport rates (pmol/h) and apparent permeability values (P_{app}) (cm/s × 10^6) were determined for each monolayer with data obtained 1 h after start of experiment using Eq. (1):

$$P_{app} = \frac{\Delta c \times V_{receiver}}{\Delta t \times C_o \times A} \tag{1}$$

where Δc is the transported amount of native resveratrol (pmol), $V_{receiver}$ is the volume of the receiver chamber (cm^3), Δt is the time interval (s), C_0 is the initial concentration of resveratrol in the donor chamber (pmol), and A is the area of the membrane (cm^2).

Kinetic parameters for metabolite secretion were estimated using Enzyme kinetics 1.0, SigmaPlot 2000 6.01, SPSS Inc., Chicago, IL for Michaelis–Menten (Eq. 2) and substrate inhibition kinetics (Eq. 3).

$$V = V_{max} \cdot S/(K_m + S) \tag{2}$$

$$V = V_{max}/(1 + K_m/S + S/K_i) \tag{3}$$

where V is the secretion rate (pmol/h), V_{max} is the maximum secretion rate, K_m is the Michaelis constant, S is the initial substrate concentration in the donor compartment (μM), and K_i the inhibition constant. The intrinsic clearance Cl_i (μl/h), which quantifies the apical and basolateral efflux of resveratrol metabolites, is defined as the ratio V_{max}/K_m.

Unless otherwise indicated, values are expressed as mean ± SD of three individual experiments. Statistical differences from control values were evaluated using the students' paired *t*-test, at a significance level of $p < 0.05$.

RESULTS

Metabolism of Resveratrol in Caco-2 Cells

Caco-2 monolayers were incubated with increasing resveratrol concentrations by applying the loading solutions (10–200 μM resveratrol) to either the apical or the basolateral chamber. Samples from both chambers were taken at the start of the experiment as well as after 1, 3 and 5 h without replacement of buffer and subsequently analyzed by HPLC. In addition to resveratrol, three metabolites M1–M3 could be detected in the apical as well as in the basolateral compartment (Fig. 1A).

Treatment of samples with β-glucuronidase prior to HPLC analysis led to the disappearance of M1 and M2 (Fig. 1B). The concomitant increase of parent resveratrol indicates glucuronidation of both metabolites. After incubation of the cytosolic samples with sulfatase, only M3 was no longer detectable, which indicates a conjugate with sulphuric acid (Fig. 1C). Negative ion mass spectra of resveratrol and
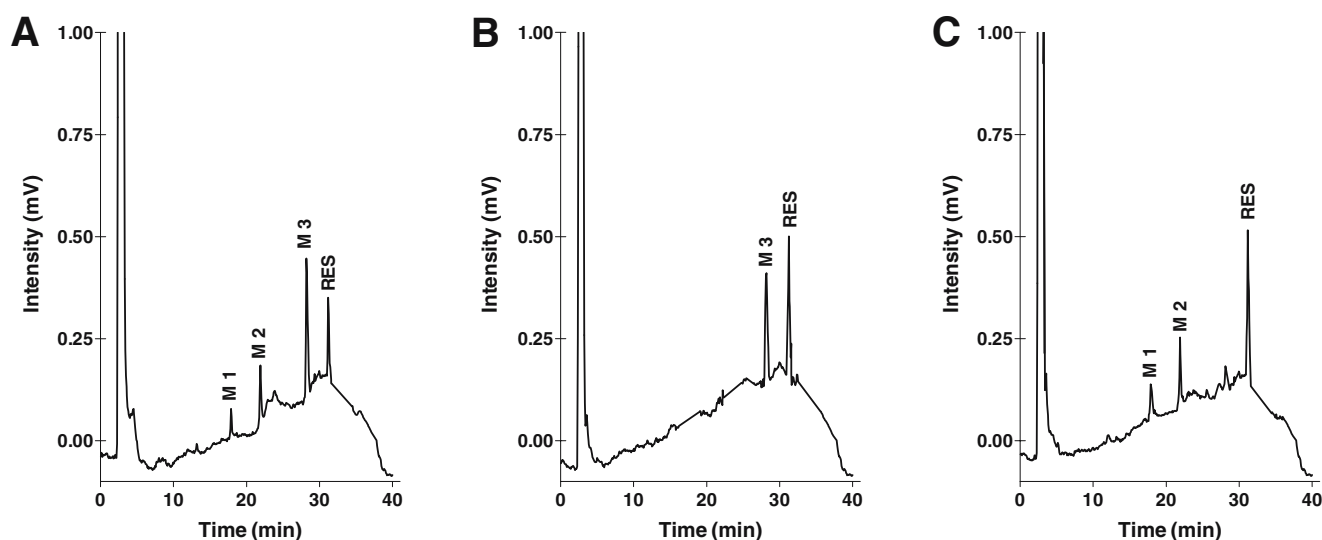
Fig. 1. Representative HPLC chromatograms of resveratrol (RES) and its metabolites M1, M2, and M3 in the basolateral compartment taken 1 h after apical loading (A) with 10 μM RES; (B) after addition of β-glucuronidase; (C) after addition of sulfatase.

its three biotransformation products showed stable molecular ions at m/z = 227, m/z = 403, m/z = 403, and m/z = 307 amu with subsequent loss of 176 amu (glucuronic acid moiety) for M1 and M2 and 80 amu (sulfuric acid moiety) for M3, in agreement with the molecular weight of resveratrol, resveratrol monoglucuronides, and resveratrol monosulfate (data not shown). Based on identical retention times and negative ion mass spectra compared to the isolated standards, the structures of M2 and M3 were confirmed as *trans*-resveratrol-3-O-glucuronide and *trans*-resveratrol-3-O-sulfate. Due to very low concentrations of M1 in Caco-2 cells and in rat bile, it was not possible to isolate a sufficient amount of this metabolite to conduct NMR experiments in order to determine the glucuronic acid group's point of attachment. However, its shorter retention time as compared to resveratrol-3-O-glucuronide (17.87 *versus* 21.35 min), strongly indicates the presence of a substituted C4′ hydroxyl group. Conjugation at the C4′ position was also supported by literature data showing a longer retention time on a reversed-phase HPLC-column for resveratrol-3-O-glucuronide based on an additional hydrogen bonding of the glucuronic acid to the -OH group at C-5, making this conjugate less polar than the resveratrol-4′-O-glucuronide (12). Based on these results, we propose that the chemical structure of M1 is a *trans*-resveratrol-4′-O-glucuronide.

Intracellular Accumulation of Resveratrol and its Metabolites

Intracellular quantification of resveratrol and its metabolites in intact Caco-2 monolayers was monitored 5 h after apical loading of resveratrol (10–200 μM), demonstrating extensive biotransformation to M1–M3. Intracellular amounts of unconjugated resveratrol increased from 370 ± 44 pmol/cm² cell layer at 10 μM resveratrol to 37,200 ± 3,220 pmol/cm² cell layer at 200 μM resveratrol, which correspond to 12 ± 1.5 and 61 ± 5.3% of total apical applied resveratrol (Table I). The intracellular concentrations of the minor biotransformation

product M1 in the cytoplasm of Caco-2 cells ranged from 8.3 ± 1.5 pmol/cm² cell layer at 10 μM resveratrol up to 104 ± 8.7 pmol/cm² cell layer at 200 μM resveratrol, which amounted only to 1.4 ± 0.25 and 0.72 ± 0.06% of apical applied resveratrol, respectively. Cytoplasmatic concentrations of the favoured glucuronide M2 were up to 30 times higher than those found for M1 (148 ± 14 pmol/cm² cell layer at 10 μM resveratrol to 2,370 ± 144 pmol/cm² cell layer at 200 μM resveratrol, representing 4.9 ± 0.62 and 2.2 ± 0.27% of total apical applied resveratrol, respectively). When 5–50 μM resveratrol were applied to the apical side of the Caco-2 cells, the formation of the sulfate conjugate M3 clearly prevailed, reaching intracellular concentrations of 440 ± 42 pmol/cm² cell layer at 10 μM, up to 1,370 ± 131 pmol/cm² cell layer at 50 μM, representing 15 ± 1.4 and 8.8 ± 0.84% of total applied resveratrol, respectively). However, using resveratrol concentrations above 50 μM, sulfation significantly declined to reach an average value of 809 ± 91 pmol/cm² cell layer at 200 μM (representing 1.9 ± 0.74% of total apical applied resveratrol).

Table I. Intracellular Accumulation of Resveratrol (RES) and its Metabolites M1–M3

RES Concentration (μM)	Concentration (pmoles/cm² cell layer)			
	M1	M2	M3	RES
10	8.3 ± 1.5	148 ± 14	440 ± 42	370 ± 44
25	19 ± 0.40	283 ± 14	1,060 ± 122	1160 ± 385
50	40 ± 4.3	1,150 ± 131	1,370 ± 131	5,960 ± 1,660
100	66 ± 5.8	1,920 ± 102	831 ± 97	14,900 ± 3,940
200	104 ± 8.7	2,370 ± 144	786 ± 88	37,200 ± 3,220

Values were calculated with data obtained 5 h after apical loading and presented as the mean ± SD (n = 3–6 monolayers).

Transport of Resveratrol Across Caco-2 Monolayers

Transport of resveratrol across the Caco-2 monolayers increased constantly for the first hour when loaded on either the apical or the basolateral side of the cells (Fig. 2). However, after 3 h the transported amount of resveratrol reached a plateau with average values ranging from 219 ± 35 to $13,400 \pm 990$ pmol after apical loading of 10 and 200 μM resveratrol, respectively. Slightly lower values were observed, when resveratrol was loaded on the basolateral side (140 ± 32 pmol at 10 μM to $8,550 \pm 971$ pmol at 200 μM).

The influence of the applied concentration on transport rates of intact resveratrol through the Caco-2 monolayers was also examined at the 1 h time point (Fig. 3). Both AP to BL and BL to AP transport rates (pmol/h) were linear up to 200 μM, indicating only a minimal contribution of carrier-mediated transport for resveratrol. There seemed to be a slight preference for the apical to basolateral flux, which may be explained by the different volumes of the apical (0.5 ml) and basolateral chamber (1.5 ml). Table II shows the corresponding apparent permeability coefficients (P_{app}), which were calculated for the first hour of incubation, when biotransformation had the lowest influence. The AP to BL

Fig. 3. The effect of applied concentration on transport rates of unconjugated resveratrol (RES) calculated after 1 h of incubation after apical and basolateral loading. Data are presented as mean ± SD ($n = 3–6$ monolayers).

permeability coefficient appeared to be concentration dependent, as it almost doubled when resveratrol concentration was increased from 10 to 50 μM, but then remained constant up to 200 μM. The basolateral to apical P_{app} values showed no significant alteration throughout the concentration range studied.

In inhibition experiments, the permeability of resveratrol was investigated in the absence and presence of verapamil, an inhibitor of P-gp, and cyclosporine, an inhibitor of P-gp and also of various MRPs. As shown in Table II, verapamil did not significantly affect the permeability of resveratrol across the Caco-2 monolayer indicating that P-gp is not involved in resveratrol transport. However, when cyclosporine was added to the apical chamber, AP to BL permeability slightly increased from 8.3 ± 1.6 to 10 ± 0.84 cm/s/10^6 indicating a minor contribution of MRPs on the apical efflux of resveratrol. No effect on resveratrol permeability was observed when cyclosporine was applied to the basolateral side (8.0 ± 2.0 to 8.6 ± 1.1 cm/s/10^6).
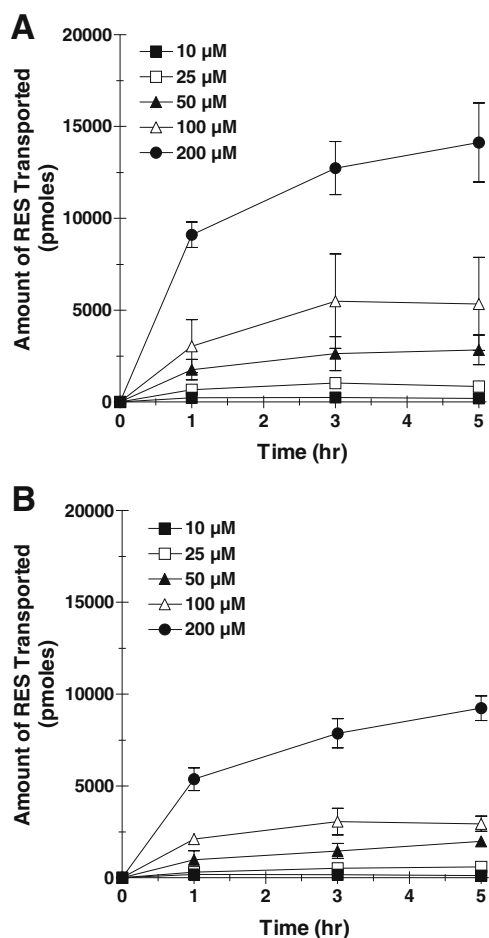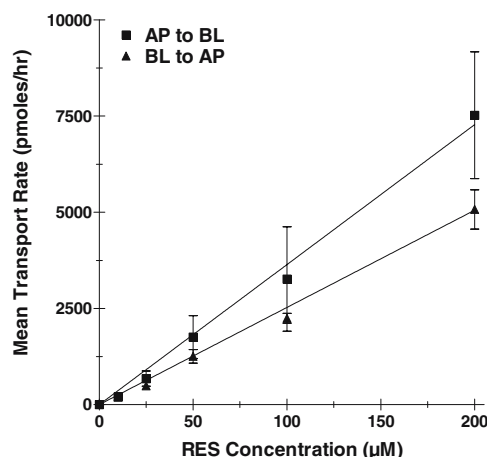

Fig. 2. The transepithelial flux of unconjugated resveratrol (RES) across the Caco-2 monolayer. (A) Apical to basolateral flux; (B) Basolateral to apical flux. Data are presented as mean ± SD ($n = 3–6$ monolayers).

Table II. Concentration-Dependent Apparent Permeability (P_{app}) of Resveratrol (RES)

RES concentration (μM)	P_{app} (cm/s/10^6)	
	AP to BL	BL to AP
10	8.3 ± 1.6	8.0 ± 2.0
25	11.9 ± 2.1	8.6 ± 0.63
50	13.9 ± 3.1	9.9 ± 0.23
100	14.2 ± 3.9	9.6 ± 1.1
200	13.6 ± 2.8	9.8 ± 0.91
10 + cyclosporine (5 μM)	10.2 ± 0.84	8.6 ± 1.1
10 + verapamil (40 μM)	8.6 ± 0.98	8.4 ± 1.1

Values are mean ± SD ($n = 3–6$ monolayers); AP to BL represents the measurements from the apical to the basolateral direction, whereas BL to AP is from the basolateral to the apical side, measured after 1 h of incubation.
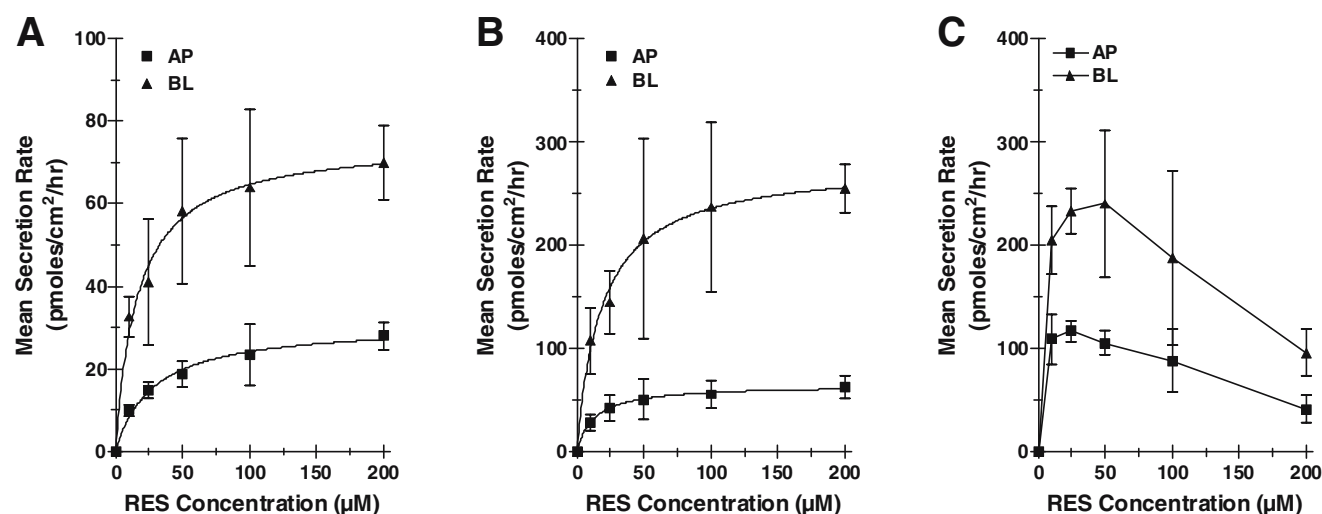
Fig. 4. The concentration dependent efflux of the resveratrol metabolites (A) M1; (B) M2; and (C) M3 into the apical and basolateral compartment after 1 h of incubation. As secretion characteristics of the metabolites are independent of loading, this figure depicts efflux after apical loading. Data are presented as mean ± SD ($n = 3–6$ monolayers).

Efflux of Resveratrol Metabolites

We also followed the efflux of the resveratrol metabolites after loading resveratrol (10–200 μM) to both the apical and basolateral side of the Caco-2 monolayers. Resveratrol underwent extensive intracellular biotransformation forming three metabolites (M1–M3), whereby all conjugates were secreted to both sides of the cell monolayer. The excreted amounts of the resveratrol sulfate M3 increased linearly with incubation time, reaching maximum values of 874 ± 302 pmol at the apical and 1580 ± 367 pmol at the basolateral side, when 10 μM resveratrol were applied to the apical side of the cells. Comparable values for M3 efflux were observed after basolateral loading with 10 μM resveratrol (711 ± 127 and 1,340 ± 100 pmol, respectively). In contrast, the efflux of the resveratrol glucuronides M1 and M2 reached a steady state after 3 h with average values of 57 ± 15 pmol for M1 and 194 ± 69 pmol for M2 at the apical and 200 ± 60 pmol for M1 and 687 ± 226 pmol for M2 at the basolateral side, when 200 μM resveratrol were applied to the apical side of the cells. Steady state rates for M1 and M2 after basolateral loading were also reached 3 h after application of 200 μM resveratrol with average rates at the apical side of 48 ± 19 pmol for M1 and 188 ± 29 pmol for M2 and 148 ± 37 pmol for M1 and 528 ± 114 pmol for M2 at the basolateral side (data not shown).

Figure 4 shows the kinetics of M1–M3 secretion into the apical and basolateral compartments, calculated after an incubation time of 60 min. The excretion of the monoglucu- ronides M1 and M2 followed classical Michaelis–Menten kinetics with significantly higher V_{max} but similar K_m values into the basolateral compartment as compared with the apical compartment (apical M1: $K_m = 28 ± 6.7$ μM, $V_{max} = 31 ± 3.9$ pmol/h; M2: $K_m = 14 ± 4.5$ μM, $V_{max} = 66 ± 4.9$ pmol/ h; basolateral: M1: $K_m = 17 ± 6.2$ μM, $V_{max} = 75 ± 6.1$ pmol/h, M2: $K_m = 19 ± 8.3$ μM, $V_{max} = 280 ± 32$ pmol/h), resulting in significantly lower apical clearance rates (V_{max}/K_m) of 1.1 ± 0.13 μl/h for M1 and 4.8 ± 1.3 μl/h for M2 compared to 4.5 ± 2.4 and 15 ± 6.1 μl/h for their basolateral efflux. Efflux of the monosulfate M3 into both compartments, however, did not follow classical Michaelis–Menten kinetics, but showed a distinct inhibition at higher resveratrol concentrations, which was now best characterized by the non-competitive substrate inhibition model (Eq. 3). The following parameters were obtained: $K_m = 27 ± 6.8$ μM, $V_{max} = 391 ± 129$ pmol/h, $V_{max}/ K_m = 14 ± 2.2$ μl/h, $K_i = 22 ± 5.3$ μM for the apical and $K_m = 16 ± 6.6$ μM, $V_{max} = 559 ± 151$ pmol/h, $V_{max}/K_m = 35 ± 6.3$ μl/ h and $K_i = 55 ± 18$ μM for the basolateral side. Similar kinetic parameters were also obtained for basolateral loading. Tables III and IV summarize the kinetic data for M1–M3 efflux in human Caco-2 cells.

DISCUSSION

The transcellular transport and metabolism of resveratrol in Caco-2 cells was investigated using an *in vitro* model of the human intestinal barrier based on Caco-2 cells cultivated

Table III. Kinetic Parameters of the Concentration-Dependent Efflux of the Resveratrol Metabolites M1–M3 after Apical Loading

	AP efflux				BL efflux			
	V_{max} (pmoles/h)	K_m (μM)	Cl_i (μl/h)	K_i (μM)	V_{max} (pmoles/h)	K_m (μM)	Cl_i (μl/h)	K_i (μM)
M1	31 ± 3.9	28 ± 6.7	1.1 ± 0.13	–	75 ± 6.1	17 ± 6.2	4.5 ± 2.4	–
M2	66 ± 4.9	14 ± 4.5	4.8 ± 1.3	–	280 ± 32	19 ± 8.3	15 ± 6.1	–
M3	391 ± 129	27 ± 6.8	14 ± 2.2	22 ± 5.3	559 ± 151	16 ± 6.6	35 ± 6.3	55 ± 18

Parameters are calculated using data obtained after 1 h of incubation and presented as the mean ± SD ($n = 3–6$ monolayers).

Table IV. Kinetic Parameters of the Concentration-Dependent Efflux of the Resveratrol Metabolites M1–M3 after Basolateral Loading

	AP efflux				BL efflux			
	V_{max} (pmoles/h)	K_m (μM)	Cl_i (μl/h)	K_i (μM)	V_{max} (pmoles/h)	K_m (μM)	Cl_i (μl/h)	K_i (μM)
M1	24 ± 2.9	17 ± 5.1	1.4 ± 0.23	–	73 ± 6.1	20 ± 6.2	3.7 ± 1.1	–
M2	53 ± 4.7	10 ± 3.3	5.3 ± 1.6	–	261 ± 28	24 ± 8.9	11 ± 4.2	–
M3	485 ± 189	30 ± 7.5	16 ± 2.9	27 ± 8.6	574 ± 135	20 ± 8.4	29 ± 5.7	77 ± 23

Parameters are calculated using data obtained after 1 h of incubation and presented as the mean ± SD ($n = 3-6$ monolayers).

in a bicameral system. Five concentrations of resveratrol (10, 25, 50, 100, and 200 μM) were chosen based on daily intakes of resveratrol as beverage (red wine) or as dietary supplement (25–50 mg/day). Resveratrol exhibited high and rapid permeability through Caco-2 monolayers. The apical to basolateral P_{app} value of $\approx 12 \times 10^{-6}$ cms^{-1} indicates good oral absorption also *in vivo* (21,22), which is consistent with recent human studies showing peak resveratrol levels already after 30–60 min and a total absorption (unconjugated and conjugated resveratrol) of about 70% based on urinary excretion data (14,15). We further conclude that passive diffusion is the major transport mechanism of resveratrol because (a) transport rates were directly proportional to applied resveratrol concentration; (b) there was no polarized transport through the monolayer, as indicated by similar AP to BL and BL to AP P_{app} values. Additionally to the passive transport, we observed a small increase of resveratrol permeability by 22% in the presence of the MRP/P-gp inhibitor cyclosporine, but not the P-gp inhibitor verapamil indicating a minor contribution of MRPs in the apical efflux of resveratrol. Our data are in accordance with very recent findings of Henry and coworkers who also found that resveratrol uses passive transport to cross the apical membrane of Caco-2 cells. These authors also demonstrate that resveratrol is a substrate of MRPs, presumably MRP2, as apical efflux of resveratrol was inhibited by the specific MRP

inhibitors MK-571 and indomethacin leading to increased intracellular accumulation of resveratrol (23). In contrast to the extensive uptake of resveratrol from the apical and basolateral medium (90–99% of the initial concentration after 5 h), only a small amount of unmetabolized resveratrol was actually transported through the Caco-2 monolayers, based on its pronounced intracellular accumulation especially at higher resveratrol concentrations (up to 61% of the initial dose at 200 μM resveratrol). Pronounced intracellular levels of native resveratrol, also observed by Kaldas *et al.* and Henry *et al.* (18,23), which may be due to high binding of the lipophilic resveratrol to intracellular proteins (24). Our data are also supported by *in vivo* findings of Vitrac *et al.*, showing high concentrations of resveratrol in the mucosa of the duodenum of living mice measured 6 h after oral administration of ^{14}C-resveratrol (25). The high accumulation of resveratrol in the Caco-2 cells emphasizes that enterocytes might be a major target site for this dietary polyphenol in the prevention of cancer and inflammatory diseases when given naturally by the oral route.

Another important factor for the low oral bioavailability of resveratrol is its extensive biotransformation (13–15). Preliminary data by Walle and coworkers, however, demonstrated a more than twofold apical to basolateral transport rate when resveratrol concentrations increased from 5 to 40 μM. No studies were done to determine whether this is due to inhibition of resveratrol conjugation. In the present work we therefore investigated the concentration-dependent formation of resveratrol conjugates in Caco-2 cells. Furthermore, the influence of biotransformation, and more importantly, the inhibition of glucuronide and sulfate formation on transepithelial transport of unconjugated resveratrol should be elucidated as any substrate inhibition of metabolites may increase oral bioavailability *in vivo*. For this purpose, all samples collected during the transport studies were simultaneously analyzed for resveratrol conjugates. Beside native resveratrol, we found three biotransformation products, namely resveratrol-4′-O-glucuronide (M1), resveratrol-3-O-glucuronide (M2) and resveratrol-3-O-sulfate (M3). Conjugation on position 4′ seems to be only a minor biotransformation pathway for resveratrol in the Caco-2 cells, as only 3.7% of 10 μM applied resveratrol were metabolized into the 4′-O-glucuronide. Clearly more favoured was glucuronidation at position 3, amounting to 12% of applied resveratrol (10 μM). However, when applied resveratrol concentration was increased further to 200 μM, M1 and M2 formation dropped to 1.3 and 4.1% of the dose, respectively. This pronounced decrease of glucuronidation may be due to a saturation of the UDP-glucuronosyltransferases UGT1A7 and UGT1A10, which are both expressed in the human
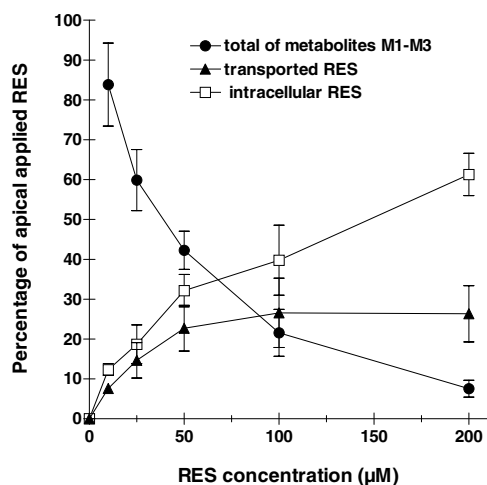

Fig. 5. The influence of metabolite (M1–M3) formation on transepithelial transport and intracellular accumulation of unconjugated resveratrol (RES). Data is calculated as percentage of the apical applied resveratrol concentration and presented as mean ± SD ($n = 3-6$ monolayers).

gastro-intestinal tract and are both able to catalyze resveratrol glucuronidation (26). Sulfation of resveratrol forming the 3-O-sulfate clearly prevailed in the lower resveratrol concentrations (10–50 μM), amounting to as much as 68% of the initial apical applied dose. However, when the initial resveratrol concentration further increased, total sulfate formation in the Caco-2 cells dropped dramatically to 2.4% of the initial applied dose (200 μM resveratrol). Kinetic analysis could further determine non-competitive substrate inhibition as the main mechanism of the observed decreased sulfate formation at higher resveratrol concentrations. This is in accordance with recent data from our lab, where we could also find in human liver cytosol that resveratrol sulfation was best characterized by the substrate inhibition model (27). Resveratrol might therefore also inhibit sulfation of other drugs as recently shown for 17β-estradiol sulfation in human mammary epithelial cells (28).

Compared to unconjugated resveratrol, intracellular accumulation of all three metabolites was significantly lower, especially at higher resveratrol concentrations. At 10 μM apical applied resveratrol, when metabolism was not saturated or inhibited, 1.4% of M1, 5.1% of M2, and 15% of M3 was retained in the cells after 5 h of incubation. These values decreased at 200 μM resveratrol apical applied down to 0.7, 2 and 1% for M1–M3, respectively. Cellular efflux of all three resveratrol conjugates clearly favoured the basolateral side of the cell layers at all concentrations tested, which was reflected in 2–4 times higher clearance rates for the basolateral efflux as compared to the apical one. This contrasts experiments performed by Kaldas and coworkers showing a higher apical efflux of resveratrol sulfate up to 20 μM resveratrol and a shift towards the basolateral side at 40 μM (18). This discrepancy may be due to the use of solid phase extraction of samples prior to HPLC-analysis as recent data from our lab showed low recovery rates for resveratrol-3-O-sufate.

The observed decrease in metabolite formation, especially that of the sulfate conjugate at higher resveratrol concentrations, may have a major impact on the oral bioavailability of resveratrol *in vivo* as saturation and inhibition of resveratrol conjugates will not only occur in the intestine but also in the liver. As can be seen in Fig. 5, the amount of transepithelial transported resveratrol is strongly dependent on its biotransformation. When 10 μM resveratrol were apical applied to the Caco-2 cells, 84 ± 10% of the initial dose were metabolized, whereas only 7.6 ± 1.2% passed the monolayers intact. Due to the observed resveratrol sulfate inhibition and the saturation of resveratrol glucuronidation, the total amount of metabolites M1–M3 decreased to 7.6 ± 1.8%, when 200 μM resveratrol were loaded to the apical side. In parallel, the total amount of unconjugated resveratrol transported from the apical chamber to the basolateral side increased to 26 ± 7.1%. These values might be even higher when taking into account the high intracellular concentration of resveratrol, which accounted for 12 ± 1.5% of total resveratrol at 10 μM and increased to 61 ± 5.3% at 200 μM. Intracellular accumulated resveratrol, strongly bound to proteins, may function as a depot, which is slowly released to the basolateral side as shown as a saturation of transported resveratrol in the high concentration range (see Fig. 5). It is not yet known whether resveratrol conjugates also exhibit

pharmacological activities. However, like the biologically inactive estrogen sulfate and glucuronide that is transformed by cellular sulfatases or by β-glucuronidase into the biological bioactive estradiol (28), resveratrol conjugates may also serve as inactive pools for resveratrol. Furthermore, conjugation might also prevent resveratrol from enzymatic oxidation, extending its half-life in the cell and maintaining its biological properties (29).

In conclusion, our data demonstrate a concentration-dependent biotransformation of resveratrol to two monoglucuronides and one monosulfate in Caco-2 cells, which may also apply to human enterocytes. The total amount of resveratrol transported from the apical to the basolateral side increased up to 3.5-fold at higher resveratrol concentrations as biotransformation is inhibited or saturated.

REFERENCES

1. J. Burns, T. Yokota, H. Ashihara, M. E. Lean, and A. Crozier. Plant foods and herbal sources of resveratrol. *J. Agric. Food Chem.* **50**:3337–3340 (2002).
2. L. Frémont. Biological effects of Resveratrol. *Life Sci.* **66**:663–673 (2000).
3. M. Jang and J. M. Pezzuto. Cancer chemopreventive activity of resveratrol. *Drugs Exp. Clin. Res.* **25**:65–77 (1999).
4. Y. J. Cai, J. G. Fang, L. P. Ma, L. Yang, and Z. L. Liu. Inhibition of free radical-induced peroxidation of rat liver microsomes by resveratrol and its analogues. *Biochim. Biophys. Acta* **1637**:31–38 (2003).
5. B. Tadolini, C. Juliano, L. Piu, F. Franconi, and L. Cabrini. Resveratrol inhibition of lipid peroxidation. *Free Radic. Res.* **33**:105–114 (2000).
6. P. Brito, L. M. Almeida, and T. C. Dinis. The interaction of resveratrol with ferrylmyoglobin and peroxynitrite; protection against LDL oxidation. *Free Radic. Res.* **36**:621–631 (2002).
7. D. Pietraforte, L. Turco, E. Azzini, and M. Minetti. On-line EPR study of free radicals induced by peroxidase/H_2O_2 in human low-density lipoprotein. *Biochim. Biophys. Acta* **1583**:176–184 (2002).
8. S. Bradamante, L. Barenghi, F. Piccinini, A. A. Bertelli, R. De Jonge, P. Beemster, and J. W. De Jong. Resveratrol provides late-phase cardioprotection by means of a nitric oxide- and adenosine-mediated mechanism. *Eur. J. Pharmacol.* **465**:115–123 (2003).
9. S. Shigematsu, S. Ishida, M. Hara, N. Takahashi, H. Yoshimatsu, T. Sakata, and R. J. Korthuis. Resveratrol, a red wine constituent polyphenol, prevents superoxide-dependent inflammatory responses induced by ischemia/reperfusion, platelet-activating factor, or oxidants. *Free Radic. Biol. Med.* **34**:810–817 (2003).
10. L. M. Hung, M. J. Su, W. K. Chu, C. W. Chiao, W. F. Chan, and J. K. Chen. The protective effect of resveratrols on ischaemia-reperfusion injuries of rat hearts is correlated with antioxidant efficacy. *Br. J. Pharmacol.* **135**:1627–1633 (2002).
11. S. Renaud and M. de Lorgeril. Wine, alcohol, platelets, and the French paradox for coronary heart disease. *Lancet* **339**: 523–1526 (1992).

12. C. Yu, Y. G. Shin, A. Chow, Y. Li, J. W. Kosmeder, Y. S. Lee, W. H. Hirschelman, J. M. Pezzuto, R. G. Mehta, and R. B. van Breemen. Human, rat, and mouse metabolism of resveratrol. *Pharm. Res.* **19**:1907–1914 (2002).

13. A. J. Gescher and W. P. Steward. Relationship between mechanisms, bioavailibility, and preclinical chemopreventive efficacy of resveratrol: a conundrum. *Cancer Epidemiol. Biomark. Prev.* **12**:953–957 (2003).

14. D. M. Goldberg, J. Yan, and G. J. Soleas. Absorption of three wine-related polyphenols in three different matrices by healthy subjects. *Clin. Biochem.* **36**:79–87 (2003).

15. T. Walle, F. Hsieh, M. H. DeLegge, J. E. Oatis Jr., and U. K. Walle. High absorption but very low bioavailability of oral resveratrol in humans. *Drug Metab. Dispos.* **12**:1377–1382 (2004).

16. X. Meng, P. Maliakal, H. Lu, M. J. Lee, and C. S. Yang. Urinary and plasma levels of resveratrol and quercetin in humans, mice, and rats after ingestion of pure compounds and grape juice. *J. Agric. Food Chem.* **52**:935–942 (2004).

17. C. De Santi, A. Pietrabissa, R. Spisni, F. Mosca, and G. M. Pacifici. Sulphation of resveratrol, a natural compound present in wine, and its inhibition by natural flavonoids. *Xenobiotica* **30**:857–866 (2000).

18. M. I. Kaldas, U. K. Walle, and T. Walle. Resveratrol transport and metabolism by human intestinal Caco-2 cells. *J. Pharm. Pharmacol.* **55**:307–312 (2003).

19. W. Jager, O. Winter, B. Halper, A. Salamon, M. Sartori, L. Gajdzik, G. Hamilton, G. Theyer, J. Graf, and T. Thalhammer. Modulation of liver canalicular transport processes by the tyrosine-kinase inhibitor genistein: implications of genistein metabolism in the rat. *Hepatology* **26**:1467–1476 (1997).

20. Y. Li, Y. G. Shin, C. Yu, J. W. Kosmeder, W. H. Hirschelman, J. M. Pezzuto, and R. B. van Breemen. Increasing the throughput and productivity of Caco-2 cell permeability assays using liquid chromatography–mass spectrometry: application to resveratrol absorption and metabolism. *Comb. Chem. High Throughput Screen.* **6**:757–767 (2003).

21. S. Yee. *In vitro* permeability across Caco-2 cells (colonic) can predict *in vivo* (small intestinal) absorption in man-fact or myth. *Pharm. Res.* **14**:763–766 (1997).

22. P. Artursson and J. Karlsson. Correlation between oral drug absorption in humans and apparent drug permeability coefficients in human intestinal epithelial (Caco-2) cells. *Biochem. Biophys. Res. Commun.* **175**:880–885 (1991).

23. C. Henry, X. Vitrac, A. Decendit, R. Ennamany, S. Krisa, and J. M. Merillon. Cellular uptake and efflux of *trans*-piceid and its aglycone *trans*-resveratrol on the apical membrane of human intestinal Caco-2 cells. *J. Agric. Food Chem.* **53**:798–803 (2005).

24. B. Jannin, M. Menzel, J. P. Berlot, D. Delmas, A. Lancon, and N. Latruffe. Transport of resveratrol, a cancer chemopreventive agent, to cellular targets: plasmatic protein binding and cell uptake. *Biochem. Pharmacol.* **68**:1113–1118 (2004).

25. X. Vitrac, A. Desmouliere, B. Brouillaud, S. Krisa, G. Deffieux, N. Barthe, J. Rosenbaum, and J. M. Merillon. Distribution of [14C]-*trans*-resveratrol, a cancer chemopreventive polyphenol, in mouse tissues after oral administration. *Life Sci.* **72**:2219–2233 (2003).

26. V. Aumont, S. Krisa, E. Battaglia, P. Netter, T. Richard, J. M. Merillon, J. Magdalou, and N. Sabolovic. Regioselective and stereospecific glucuronidation of *trans*- and *cis*-resveratrol in human. *Arch. Biochem. Biophys.* **393**:281–289 (2001).

27. M. Miksits, A. Maier-Salamon, S. Aust, T. Thalhammer, G. Resnicek, O. Kunert, E. Haslinger, T. Szekeres, and W. Jäger. Sulfation of resveratrol in human liver: evidence of a major role for the sulfotransferases SULT1A1 and SULT1E1. *Xenobiotica* **35**:1101–1119 (2005).

28. Y. Otake, A. L. Nolan, U. K. Walle, and T. Walle. Quercetin and resveratrol potently reduce estrogen sulfotransferase activity in normal human mammary epithelial cells. *J. Steroid Biochem. Mol. Biol.* **73**:265–270 (2000).

29. J. R. Pasqualini and G. S. Chetrite. Recent insight on the control of enzymes involved in estrogen formation and transformation in human breast cancer. *J. Steroid Biochem. Mol. Biol.* **93**:221–236 (2005).

30. G. Regev-Shoshani, O. Shoseyov, I. Bilkis, and Z. Kerem. Glycosylation of resveratrol protects it from enzymic oxidation. *Biochem. J.* **374**:157–163 (2003).